The American Journal of Pathology, Vol. 174, No. 5, May 2009

DOI: 10.2353/ajpath.2009.080709

Cell Injury, Repair, Aging and Apoptosis

Inhibition of Prostaglandin D Synthase Suppresses Muscular Necrosis

Ikuko Mohri,*†‡ Kosuke Aritake,‡ Hidetoshi Taniguchi,† Yo Sato,‡ Shinya Kamauchi,‡ Nanae Nagata,‡ Toshihiko Maruyama,‡ Masako Taniike,*† and Yoshihiro Urade‡

From the Department of Mental Health and Environmental Effects Research, Molecular Research Center for Child Mental Development, and the Department of Developmental Medicine (Pediatrics),† Osaka University Graduate School of Medicine, Osaka; and the Department of Molecular Behavioral Biology,‡ Osaka Bioscience Institute, Osaka, Japan*

Duchenne muscular dystrophy is a fatal muscle wasting disease that is characterized by a deficiency in the protein dystrophin. Previously, we reported that the expression of hematopoietic prostaglandin D synthase (HPGDS) appeared in necrotic muscle fibers from patients with either Duchenne muscular dystrophy or polymyositis. HPGDS is responsible for the production of the inflammatory mediator, prostaglandin D_2. In this paper, we validated the hypothesis that HPGDS has a role in the etiology of muscular necrosis. We investigated the expression of HPGDS/prostaglandin D_2 signaling using two different mouse models of muscle necrosis, that is, bupivacaine-induced muscle necrosis and the *mdx* mouse, which has a genetic muscular dystrophy. We treated each mouse model with the HPGDS-specific inhibitor, HQL-79, and measured both necrotic muscle volume and selected cytokine mRNA levels. We confirmed that HPGDS expression was induced in necrotic muscle fibers in both bupivacaine-injected muscle and *mdx* mice. After administration of HQL-79, necrotic muscle volume was significantly decreased in both mouse models. Additionally, mRNA levels of both CD11b and transforming growth factor β1 were significantly lower in HQL-79-treated *mdx* mice than in vehicle-treated animals. We also demonstrated that HQL-79 suppressed prostaglandin D_2 production and improved muscle strength in the *mdx* mouse. Our results show that HPGDS augments inflammation, which is followed by muscle injury. Furthermore, the inhibition of HPGDS ameliorates muscle necrosis even in cases of genetic muscular dystrophy. ***(Am J Pathol 2009, 174:1735–1744; DOI: 10.2353/ajpath.2009.080709)***

Duchenne muscular dystrophy (DMD) is one of the most common types of muscular dystrophy, affecting approximately 1 out of 3500 boys.[1] Progressive muscular dystrophy in DMD is caused by membrane vulnerability,[2] which results from a defect in the muscle protein dystrophin,[3,4] but the precise pathophysiology of the disease progression is not known. There is still no complete cure for this disastrous disease, albeit gene transfer has been extensively tried in mammalian models. Glucocorticoids[5,6] and their analogs[7] are effective in suppressing the disease only to some degree. In DMD, these steroids reduce the infiltration of inflammatory cells into the muscle[8] and down-regulate the expression of genes involved in the immune response.[9] These data suggest inflammation may play a role in the progression of the disease.

Earlier we reported the expression of hematopoietic prostaglandin (PG) D synthase (HPGDS), the enzyme responsible for the production of PGD_2,[10] in necrotic muscle fibers, mainly in the focus of grouped necrosis, in patients with DMD or polymyositis.[11] We recently reported that overproduction of PGD_2 produced by HPGDS aggravates inflammation and causes profound tissue damage in *twitcher*, a genetic demyelinating mouse mod-

Supported in part by research grants from Japan Applied Enzymology (to I.M., Y.U. and K.A); Takeda Science Foundation (to Y.U.); Mitsubishi Foundation (to Y.U.); the Ministry of Education, Culture, Sports, Science, and Technology of Japan (09670806 to M.T. and 19591205 to I.M. 19590094 to K.A.), The Morinaga Foundation for Health & Nutrition (to M.T.); the Osaka Medical Research Foundation for Incurable Diseases (to M.T.); Program for Promotion of Fundamental Studies in Health Science of the National Institute of Biomedical Innovation (to Y.U.); The Research Grant (19A-1) for Nervous and Mental Disorders from the Ministry of Health, Labor and Welfare (to Y.U.); and Osaka City.

Accepted for publication January 27, 2009.

Address reprint requests to Yoshihiro Urade, PhD, Department of Molecular Behavioral Biology, Osaka Bioscience Institute, Furuedai 6-2-4, Suita, Osaka, 565-0874, Japan., E-mail: uradey@obi.or.jp; or Masako Taniike, MD, PhD, Department of Mental Health and Environmental Effects Research, The Molecular Research Center for Child Mental Development, Osaka University Graduate School of Medicine, 2–2, Yamadaoka, Suita, Osaka 560-0871, Japan, E-mail: masako@ped.med.osaka-u.ac.jp.

el.[12] The biosynthesis of PGs was also suppressed by glucocorticoids, via suppression of enzymes in the overall synthesis of PGs including phospholipase A_2 and cyclooxygenase. PGD_2 mediates inflammatory responses through two specific receptors, DP1[13] and DP2,[14] causing peripheral vasodilatation, augmentation of vascular permeability, and chemotaxis.[15] Based on these findings, we hypothesized that HPGDS augments the inflammation that is followed by the muscle injury, especially in the foci of grouped necrosis. Here, using bupivacaine hydrochloride (BPVC)-induced muscle necrosis, where sequences of muscle necrosis are similar to that of progressive muscular dystrophy,[16] and the *mdx* mouse as a DMD model, we clarified the role of PGD_2 in the pathogenesis and investigated the therapeutic potentials of blockade of HPGDS/PGD_2/DP signaling on the muscular necrosis.

Materials and Methods

Mice

All animal experiments were performed in accordance with the Japanese Law for the Protection of Experimental Animals and conformed to the regulations issued by the National Institutes of Health and the Society for Neuroscience. We used the C57BL/6 mouse strain for the BPVC-induced muscular necrosis model. Human HPGDS (hHPGDS)-TG mice were generated on an FVB background as described before.[17] Wild-type mice of the FVB strain were used as controls for the experiments using hHPGDS-TG mice.

The *mdx* mice (C57BL/10 ScSn, JAX Laboratories) were a generous gift from Dr. Shin'ichi Takeda (Dept of Molecular Therapy, National Institute of Neuroscience, National Center of Neurology and Psychiatry, Kodaira, Tokyo, Japan), and the mutation was maintained by interbreeding.

BPVC-Induced Mouse Model

This study was conducted with 7-week-old male mice as described previously.[16,18] Under deep anesthesia, 0.05 ml of 0.1% BPVC was injected into the exposed quadriceps muscle under direct vision. As the control, the quadriceps muscles of mice were received 0.05 ml of sterile saline in the same manner.

Mice in the BPVC group were randomly assigned to two subgroups and treated in a double-blind manner with vehicle (0.5% methyl cellulose, $n = 8$) or an HPGDS inhibitor (HQL-79; 30 mg/kg/day in 0.5% methyl cellulose, $n = 10$)[19] orally, 1 hour before and every 24 hours, until 7 days after the BPVC injection. In case of treatment with a specific antagonist for DP1 (BW A868C; Cayman, Ann Arbor, MI)[20] or DP2 (Ramatroban; Cayman),[21] mice were subcutaneously injected 1 hour before and every 24 hours until 7 days after the BPVC injection. BW A868C and Ramatroban are chemical compounds that respectively bind to DP1[20] and DP2[21] receptors for PGD_2 and inhibit their signal transduction at the expression sites.

The mdx Mouse Model

Wild-type C57BL/10 ScSn mice were used as the control. Male *mdx* mice at 4 weeks of age were randomly assigned to 2 groups and treated in a double-blind manner with vehicle (0.5% methyl cellulose) or an HPGDS inhibitor (HQL-79; 30 mg/kg/day in 0.5% methyl cellulose) orally for 10 days.

Muscle Pathology and Immunocytochemistry

Removed muscles were immersed overnight at 4°C in 4% paraformaldehyde in 0.1 M/L sodium phosphate (pH 7.4) and processed into paraffin blocks. Both paraffin and frozen sections (5 μm thick) were mounted on 3-aminopropyltriethoxysilane-coated slides. Some serial paraffin sections were routinely stained with H&E, and others were immunostained for HPGDS; and frozen sections were immunostained for DP1 as previously described.[22,23]

Western Blot Analysis

The muscle was homogenized in 3 volumes of PBS by weight. After centrifugation at 16,000 $\times$ *g* for 20 minutes, the resultant supernatant was used for Western blotting of HPGDS. Protein (10 μg/lane) was separated by SDS-polyacrylamide gel electrophoresis, transferred to an Immobilon PVDF membrane (Millipore, Bedford, MA), and immunostained as described earlier.[22]

Quantitative PCR

Total RNA was extracted from mouse quadriceps by the guanidinium thiocyanate-phenol-chloroform method using ISOGEN (Nippon Gene, Tokyo, Japan). The quantitative PCR analyses of the contents of mRNAs for HPGDS, DP1, DP2, CD11b (a surface antigen expressed on macrophages and granulocytes[24,25]), tumor necrosis factor (TNF)α, transforming growth factor (TGF)β1, and glyceraldehyde-3-phosphate dehydrogenase were performed by using the LightCycler amplification and detection system (Roche Diagnostics, Indianapolis, IN) as described below. The sequence-specific primers used were as follows: HPGDS forward primer, 5′-GAATAGAACAAGCTGACTGGC-3′; HPGDS reverse primer, 5′-AGCCAAATCTGTGTTTTTGG-3′; DP1 forward primer, 5′-TTTGGGAAGTTCGTGCAGTACT-3′; DP1 reverse primer, 5′-GCCATGAGGCTGGAGTAGA-3′; DP2 forward primer, 5′-TGGCCTTCTTCAACAGCGT-3′; DP2 reverse primer, 5′-ACGCAGTTGGGGAATTCG-3′; CD11b forward primer, 5′-CAGGGACAACCACACCTCTTG-3′; CD11b reverse primer, 5′-GCAGCGTCATACCAGCACAC-3′; TNFα forward primer, 5′-AGTGACAAGCCTGTAGCCCACG-3′; TNFα reverse primer, 5′-TTTCTCCTGGTATGAGATAGC-3′; TGFβ1 forward primer, 5′-TGCGCTTGCAGAGATTAAAA-3′; TGFβ1 reverse primer, 5′-AGCCCGAAGCGGACTACTAT-3′;

glyceraldehyde-3-phosphate dehydrogenase forward primer, 5′-TGAACGGGAAGCTCACTGG-3′; and glyceraldehyde-3-phosphate dehydrogenase reverse primer, 5′-TCCACCACCCTGTTGCT-3′.

All mRNA levels are shown after normalization with the mRNA level of glyceraldehyde-3-phosphate dehydrogenase. The constructs used to create a standard curve were made by cloning each amplified fragment into the HindIII site of a pGEM vector (Promega, Madison, WI). All PCR products were visualized under UV light after electrophoresis in an agarose gel containing ethidium bromide and were subsequently sequenced to verify that only the specific polymerization from the intended mRNA had occurred.

Estimation of the Volume of Necrotic Muscle by Injecting Evans blue dye

Evans Blue dye (10 mg/ml PBS, Sigma, St. Louis, MO) was injected intravenously into a tail vein of mice (50 μl per 10 g body weight) as described previously.[26,27] The animals were sacrificed 4 hours after the injection. Muscles were removed, frozen on dry ice and lyophilized. Evans blue dye in the muscles was extracted by formamide (Nakalai Tesque, Kyoto, Japan) at 60°C overnight. The amount of Evans blue dye in the extract was quantified with an absorption spectrometer at 630 nm, and with external standards ranging from 10 to 1000 ng/ml.

Computed Tomography Scan Analysis

The volume of necrotic muscle was visualized radiographically by using a LaTheta X-ray computed tomography (CT, ALOKA, Tokyo, Japan) according to the manufacturer's protocol. Anesthetized mice were scanned in the dorsal position 15 minutes during an intravenous infusion via a distal tail vein of a non-ionic contrast medium (Iopamiron, Bayer, Osaka, Japan) at the infusion rate of 1.2 ml/hr.

The CT scan image data from each mouse were analyzed by visualization software (ALOKA), which displayed the data as 2D axial cross-sectional images. We confirmed a linear correlation of the necrotic volume between the X-ray CT analysis and the estimation of the volume of necrotic muscle made by using Evans blue dye injection (data not shown). The three-dimensional data were constructed from sliced CT images by summing those images along the Z-axis by using VGStudio MAX software (Volume Graphics, Heidelbelg, Germany).

Measurement of Urinary PGD_2 Metabolite

11,15-Dioxo-9-hydroxy-2,3,4,5-tetranorprostan-1,20-dioic acid (tetranor-PGDM) was identified by mass spectrometry as a metabolite of infused PGD_2 that is detectable in mouse and human urine.[28] Daily urine was collected from wild-type mice and *mdx* mice, and the amount of tetranor-PGDM in it was determined by using liquid chromatography-tandem mass spectrometry as previously described.[28] The creatinine concentration was measured by assay kit (Wako Pure Chemical, Osaka, Japan).

Grip Strength Test

Grip strength was assessed with a grip strength meter consisting of a horizontal forelimb mesh (Brain Science Idea, Osaka, Japan). Five successful forelimb strength measurements within 2 minutes were recorded. The average values of each day were used for subsequent analysis. The grip strength measurements were collected in the morning hours.

Statistical Analysis

Values were expressed as the mean ± SE. Data were analyzed by using the 2-tailed *t*-test, and values $P < 0.05$ were considered to be significant.

Results

$HPGDS^+$ Immunoreactivity Recognized in the Necrotic Fibers in BPVC-Induced Muscular Necrosis

Figure 1 illustrates the temporal alteration in HE staining and HPGDS immunocytochemistry at 6 hours, and 2 and 4 days after a BPVC injection into mice (C57BL/6 strain). H&E staining revealed obvious muscle injury at 6 hours (Figure 1A), which reached its peak at day 2 (Figure 1B) when numerous infiltrating cells (arrows in Figure 1B) were found surrounding the necrotic fibers. At day 4 after the BPVC injection, eosinophilic regenerating fibers were increased in number (Figure 1C, arrowsheads) and their diameter enlarged. The necrotic fibers were almost completely replaced by regenerated fibers by day 7. HPGDS-immunoreactivity was not observed in the muscle fibers before or 6 hours after the BPVC injection (Figure 1D), but it was detected at day 1 and after (Figure 1, E and F) in the necrotic muscle. The number of HPGDS-positive necrotic fibers reached a peak at day 2 (Figure 1E). There were many HPGDS-positive macrophages observed at day 2 and 4 (arrows in Figure 1, E and F). Weak HPGDS immunoreactivity was also observed in eosinophilic regenerating fibers during the early phase of regeneration (Figure 1 F, arrows). At day 7, regenerating muscle fibers were well enlarged, and HPGDS immunoreactivity had diminished (data not shown). Western blotting (Figure 1G) revealed that HPGDS protein was induced in both BPVC- and saline-injected muscle at 6 hours; however, its level decreased quickly in the case of the saline injection but increased after BPVC injection with a peak at day 2 and gradually decreased thereafter. DP1 immunoreactivity was also observed in the necrotic fibers at day 2 (Figure 1H), as in the case of HPGDS indicated above. Figure 1, I–L shows the expression profile of mRNAs for HPGDS, CD11b (a marker for infiltrating macrophages), DP1, and DP2 as determined by quantitative reverse transcription (RT)-PCR. The lavels of both HPGDS and

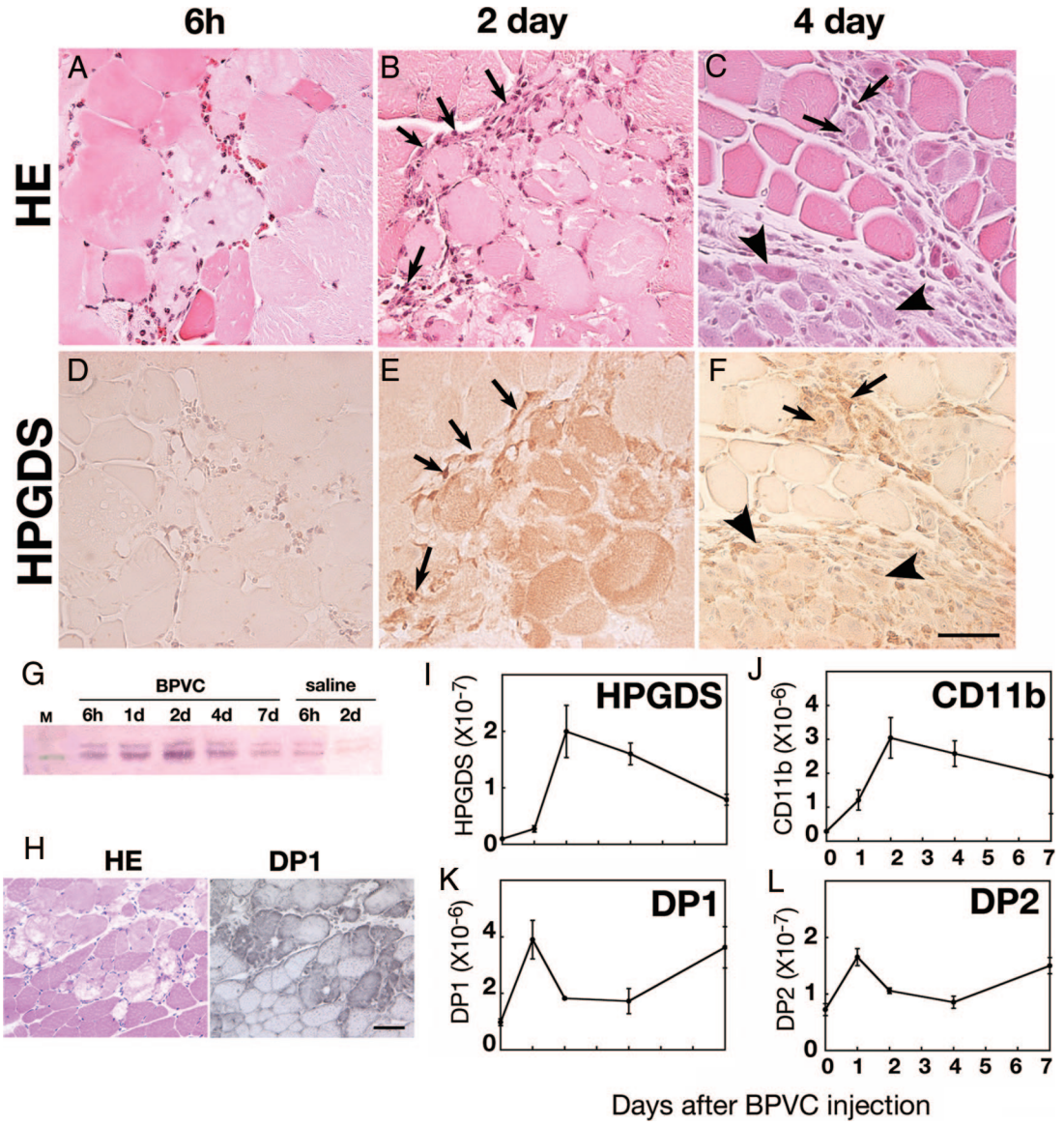

Figure 1. A–H: HPGDS expression in necrotic muscle fibers. Results of HE staining (**A–C**) and HPGDS immunostaining (**D–F**) at 6 hour (**A, D**), 2 days (**B, E**), and 4 days (**C, F**) after BPVC injection. Scale bar = 50 μm. **Arrows** and **arrowheads** indicate HPGDS-positive infiltrating macrophages and regenerating muscle fibers, respectively. **G:** Western blotting for HPGDS. **H:** DP1 expression in necrotic muscle fibers. Left, HE staining; right, DP1 immunocytochemistry. Scale bar = 50 μm. **I–L:** Quantitative RT-PCR for mRNAs of HPGDS (**I**), CD11b (**J**), DP1 (**K**), and DP2 (**L**). $n = 4$. Data are the mean ± SE.

CD11b mRNAs increased after the BPVC injection, reached their peak at day 2, and thereafter gradually decreased (Figure 1, I and J, respectively). On the other hand, both DP1 and DP2 mRNAs showed a bimodal expression pattern with peaks at day 1 and day 7 (Figure 1, K and L, respectively).

HPGDS-Overexpression Exacerbated Muscle Necrosis

We hypothesized that PGD_2 produced by HPGDS in the muscle injury aggravated the muscular necrosis in the BPVC-induced muscular necrosis model. To evaluate this possibility, we compared the BPVC-induced muscular necrosis between wild-type mice and human HPGDS-overexpressing transgenic (hHPGDS-TG) mice[17] of the same genetic background (FVB strain), which constitutively express a large amount of human HPGDS in addition to endogenous mouse HPGDS (Figure 2, A and B). As shown in Figure 2A, H&E staining revealed that massive muscular necrosis occurred at day 2 in the BPVC-injected hHPGDS-TG mice; and there were wide interfiber spaces in the muscle, suggesting severe edema. When compared with that in the control muscles, the muscle necrosis in the hHPGDS-TG mice was exaggerated and prolonged. As shown in Figure 2B, the relative water content was significantly higher in the hHPGDS-TG mouse muscle than in the wild-type one at 2 days after the BPVC injection. These results indicate that overproduction of PGD_2 augmented the muscle necrosis and edema.

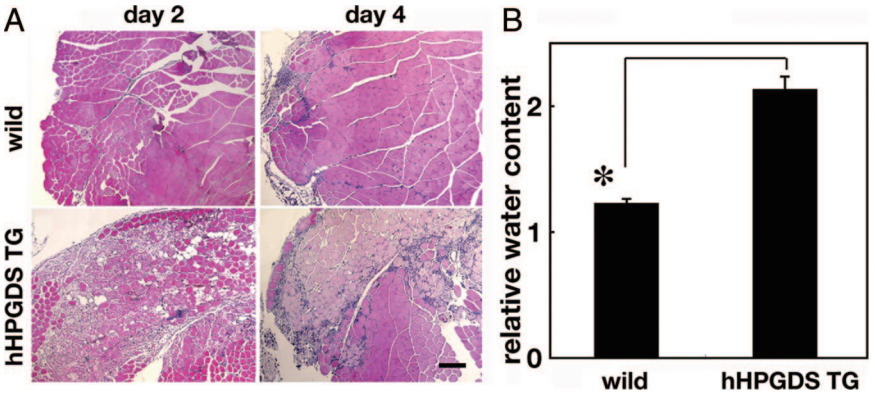

Figure 2. PGD$_2$ overproduction augments muscle necrosis. **A:** Result of H&E staining of the quadriceps muscle of wild-type and human HPGDS-TG mice obtained at 2 and 4 days after the injection of BPVC. Scale bar = 50 μm. **B:** Comparison of the water content in the muscle between wild-type and human HPGDS-TG mice at 2 days after the BPVC injection. The water content is shown as the value relative to that of control mice. $n = 4$ in each group. Data are the mean ± SE. $^*P < 0.05$.

HPGDS Inhibitor Ameliorated Muscle Necrosis in the BPVC-Induced Model

Next we treated BPVC-injected mice with HQL-79, a specific inhibitor of HPGDS.[19,29,30] Mice were orally administrated 30 mg/kg/day of HQL-79 1 hour before the BPVC injection and then once a day for 7 days after it. The volume of necrotic muscle and severity of necrosis were evaluated by Evans blue dye leakage and cell infiltration. As shown in Figure 3A, the necrotic muscle volume evaluated by the use of Evans blue dye was increased after BPVC injection and peaked at day 2 in both vehicle-treated mice and HQL-treated mice. However, from day 2 the volume was lower in the HQL-79-treated mice than in the vehicle-treated ones. At day 4, the volume of muscle necrosis was significantly reduced to 70% of the control by the HQL-79 treatment ($P < 0.05$, Figure 3A). At day 7, the amount of Evans blue dye within the muscle returned to the level before BPVC administration. We also determined, by quantitative RT-PCR, the mRNA level of CD11b, a marker for inflammatory cells, to monitor the accumulation of macrophages that had infiltrated into the necrotic muscle fibers (Figure 3B). The content of CD11b mRNA rapidly increased after the BPVC injection, peaked at day 2, and then slowly became reduced in the vehicle-treated mice. In the HQL-79-treated mice, the content also rapidly increased after the BPVC injection, peaked at day 2, but then decreased more rapidly after day 2 than that in the vehicle-treated mice. At day 4, the CD11b mRNA level in the HQL-79-treated mice was significantly ($P < 0.01$) reduced to less than 50% of that in the vehicle-treated mice. These results, taken together, indicate that inhibition of HPGDS by HQL-79 decreased both the muscular necrosis and the infiltration of inflammatory cells.

As was shown in Figure 1, the mRNA levels of both receptors for PGD$_2$, ie, DP1 and DP2, were up-regulated in the necrotic muscle. To examine whether either or both of these receptors were involved in the muscle necrosis, we administered an antagonist specific for DP1 (BW

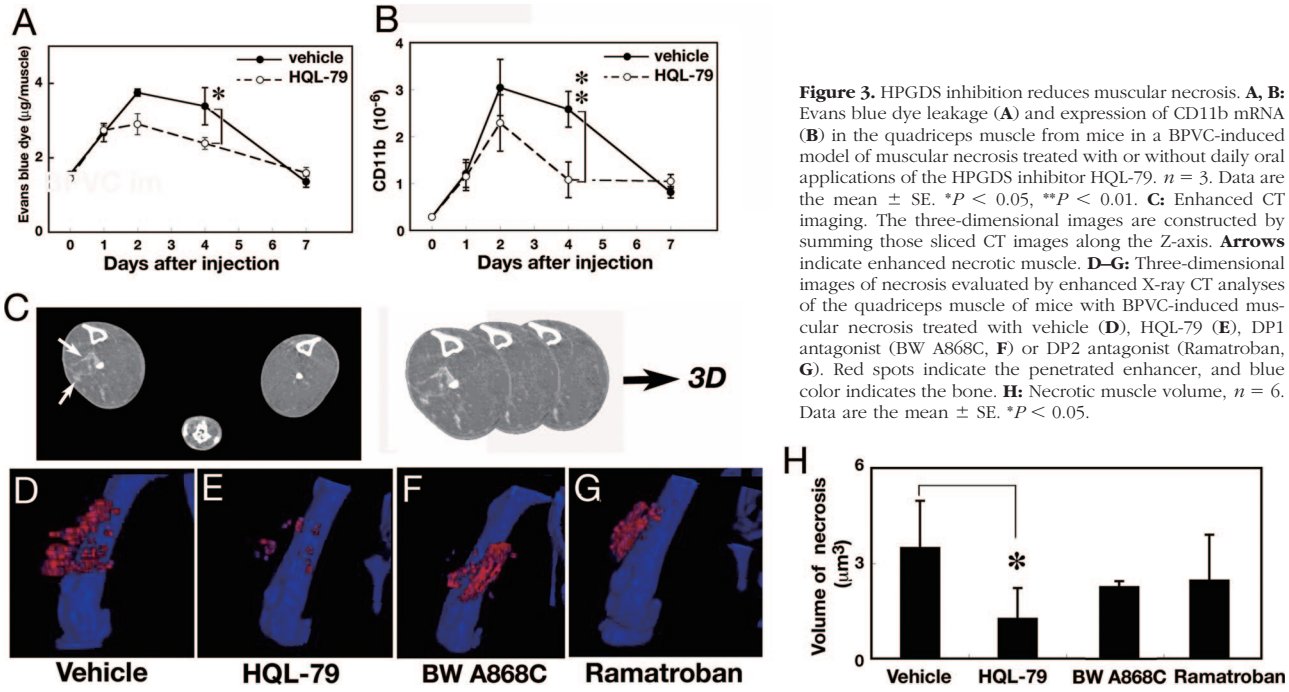

Figure 3. HPGDS inhibition reduces muscular necrosis. **A, B:** Evans blue dye leakage (**A**) and expression of CD11b mRNA (**B**) in the quadriceps muscle from mice in a BPVC-induced model of muscular necrosis treated with or without daily oral applications of the HPGDS inhibitor HQL-79. $n = 3$. Data are the mean ± SE. $^*P < 0.05$, $^{**}P < 0.01$. **C:** Enhanced CT imaging. The three-dimensional images are constructed by summing those sliced CT images along the Z-axis. **Arrows** indicate enhanced necrotic muscle. **D–G:** Three-dimensional images of necrosis evaluated by enhanced X-ray CT analyses of the quadriceps muscle of mice with BPVC-induced muscular necrosis treated with vehicle (**D**), HQL-79 (**E**), DP1 antagonist (BW A868C, **F**) or DP2 antagonist (Ramatroban, **G**). Red spots indicate the penetrated enhancer, and blue color indicates the bone. **H:** Necrotic muscle volume, $n = 6$. Data are the mean ± SE. $^*P < 0.05$.

A868C; 1 mg/kg or DP2 (Ramatroban, 5 mg/kg) 1 hour before the BPVC injection and then once a day for 7 days and compared their effects on the expansion of muscular necrosis with that effect of HQL-79 by conducting enhanced X-ray CT analysis after infusion of a non-ionic contrast medium. We confirmed a linear correlation between the necrotic volume determined by the X-ray CT and the estimation of the volume of necrotic muscle made by using the Evans blue dye injection. Figure 3C explain how to construct the 3D images of muscular necrosis.

Figures 3D-G represent the reconstructed 3D images of enhanced CT of BPVC-injected mice at day 4 after treatment with vehicle, HQL-79, BW A868C or Ramatroban, respectively, in which the damaged muscle containing the non-ionic contrast medium is shown in red. The calculated necrotic muscle volume at day 4 was significantly reduced in mice treated with HQL-79, but not in those given the DP1 or DP2 antagonist (Figure 3H). These results indicate that the HPGDS inhibitor was more effective to reduce the muscle necrosis than either DP1 or DP2 antagonist alone and that PGD_2 signaling exerted its function via both DP1 and DP2 receptors in muscular necrosis.

HPGDS-Immunoreactive Fibers Recognized in the Foci of Grouped Necrosis in mdx *Mouse Muscle*

We then examined the immunocytochemical distribution of HPGDS expression in the *mdx* mouse, which is an authentic mouse model of DMD caused by defective dystrophin molecules. As shown in Figure 4A and B, many HPGDS-positive fibers were observed in *mdx* mouse muscles, which fibers were often clustered and identified to be necrotic as compared with those in an H&E-stained adjacent section, as seen similarly in DMD as described before[11] (Figure 4, A and B). Higher magnification views disclosed that HPGDS expression was hardly seen in opaque fibers (Figure 4, C and D) but was strong in the ballooned hyaline-like fibers without (Figure 4, E and F) or with (Figure 4, G and H) cellular infiltration. Infiltrating macrophages also expressed HPGDS (arrowheads in Figure 4, G, I, H, L). At the last stage, the necrotic muscle was replaced with HPGDS-positive macrophages (arrowheads in Figure 4, I and J) and regenerating muscle fibers (arrows in Figure 4, I and J). When we quantified the number of HPGDS-expressing fibers at each stage of degeneration, HPGDS-immunoreactivity was not detected in the opaque fibers but was detected in 97% of the ballooned hyaline-like fibers without cell infiltration, 95% of those with cellular infiltration, and 60% of the regenerating fibers of *mdx* mice. Quantitative RT-PCR revealed that the contents of HPGDS, DP1, and DP2 mRNAs were significantly higher in the 4-week-old *mdx* mice than in the wild-type mice (Figure 4, K–M).

HQL-79 Treatment Reduced the Muscular Necrosis in mdx *Mice*

To examine whether HQL-79 could reduce the muscle necrosis in the *mdx* mouse as it did in the BPVC-induced muscle necrosis model, we treated *mdx* mice with HQL-79 and analyzed their muscles by enhanced X-ray CT analysis after infusion of the non-ionic contrast medium. Based on the 3D-images constructed from the sliced CT images, we monitored the changes in the necrotic muscular volume of each *mdx* mouse before and after oral administration of vehicle or HQL-79 daily for 5 days. Figure 5A shows the typical three-dimensional images of an *mdx* mouse before and after oral administration of vehicle or HQL-79, in which the damaged muscle containing the non-ionic contrast medium is shown in red. The positions of the necrotic muscle fibers (red in Figure 5A) changed during the 5-day period in both *mdx* mice. The total necrotic volume was almost unchanged in the vehicle-treated mouse but remarkably decreased in the HQL-79-treated mouse. Figure 5B (left panel) shows the change in the volume of necrotic muscle fibers in each of several *mdx* mice before and after daily treatment with vehicle and HQL-79 for 5 days. The necrotic muscle volume increased in 5 out of the 9 vehicle-treated mice; however, it decreased in all HQL-79-treated mice except one. As summarized in Figure 5B (right panel), treatment with HQL-79 significantly ($P < 0.05$) reduced the necrotic muscle volume in the *mdx* mice.

To confirm the effect of HQL-79, we determined the mRNA contents of CD11b, HPGDS, DP1, DP2, and two types of proinflammatory cytokines, TNFα and TGFβ1, in wild-type mice and *mdx* mice treated with vehicle or HQL-79 for 10 days, by quantitative RT-PCR (Figure 5, C–H). As compared with those of the wild-type mice, the levels of mRNAs for CD11b, HPGDS, DP1, and DP2 were significantly increased in the *mdx* ones (Figure 5, C–F). The mRNA levels of CD11b, HPGDS, and DP2 were significantly decreased after HQL-79 treatment in *mdx* animals ($P < 0.05$, Figure 5, C–F). The levels of proinflammatory cytokines TNFα and TGFβ1 were also significantly increased in *mdx* muscles (Figure 4, G and H, $P < 0.05$). HQL-79 treatment significantly ($P < 0.05$) decreased the TGFβ1, but not the TNFα, mRNA in the *mdx* mice.

To confirm the functional significance of the inhibition by HQL-79, we measured the level of tetranor-PGDM, a PGD_2 metabolite, in the urine of *mdx* mice before and after HQL-79 administration. The urinary level of tetranor-PGDM was about 3 times higher in the *mdx* (17.8 $\pm$ 0.8 ng/mg Cre, mean $\pm$ SE) than in the wild-type mice (6.8 $\pm$ 1.0; $P < 0.0003$). As shown in Figure 5I, HQL-79 administration to *mdx* mice for 5 days significantly ($P < 0.0003$) decreased the amount of urinary tetranor-PGDM from 12.4 $\pm$ 1.4 to 4.2 $\pm$ 0.4 (ng/mg Cre), which was slightly lower than the level for the wild-type mice. These results indicate that the PGD_2 production was increased in the *mdx* mice and that HQL-79 suppressed the PGD_2 production by HPGDS up-regulated in these animals.

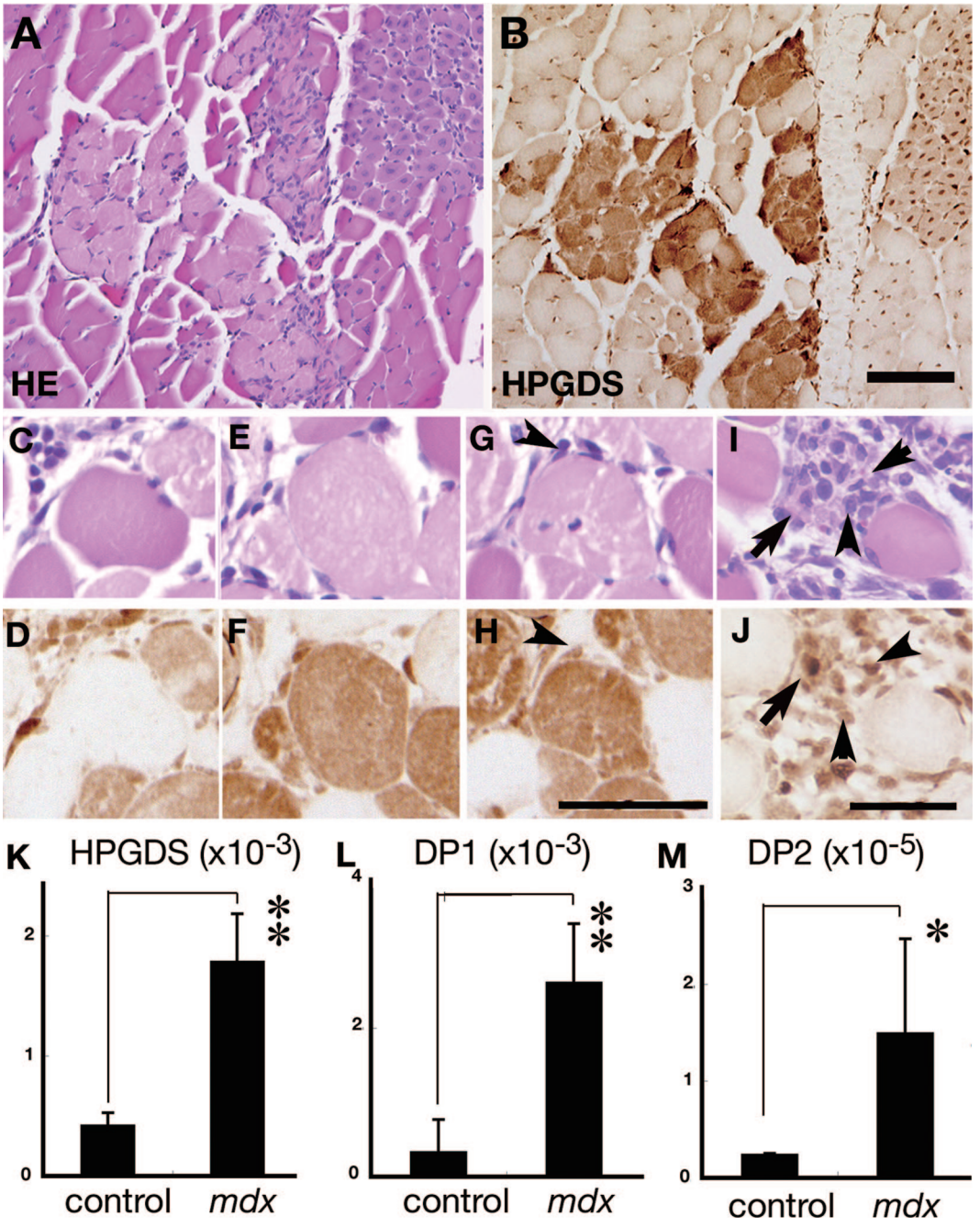

Figure 4. HPGDS expression in the necrotic muscle from an *mdx* mouse. **A, C, E, G, I:** H&E staining. **B, D, F, H, J:** HPGDS immunocytochemistry. Scale bar = 50 μm. **Arrowheads** indicate HPGDS-positive macrophages; and **arrows**, HPGDS-positive regenerating muscle fibers. **K–M:** Quantitative RT-PCR for HPGDS, DP1, and DP2 mRNAs. $n = 4$. Data are the mean ± SE. $^{*}P < 0.05$, $^{**}P < 0.01$.

Furthermore, to examine the clinical response of *mdx* mice to HQL-79, we performed a forelimb grip strength test by using an automated grip strength meter. As shown in Figure 5J, the grip strength in the HQL-79-treated *mdx* mice (180.9 ± 16.3 g/sec; mean ± SE) was significantly increased by the inhibitor compared with that for the vehicle-treated ones (132.9 ± 10.7 g/sec; $P < 0.05$). These results demonstrate that HQL-79 improved the clinical symptom of muscular dystrophy in *mdx* mice.

Discussion

Significance of HPGDS Expression in the Hyalinated Necrotic Fibers in the Foci of Grouped Necrosis

In this study, we showed that HPGDS was expressed in the necrotic muscular fibers in both BPVC-induced and *mdx* mouse models in a stage-specific manner. In both BPVC-

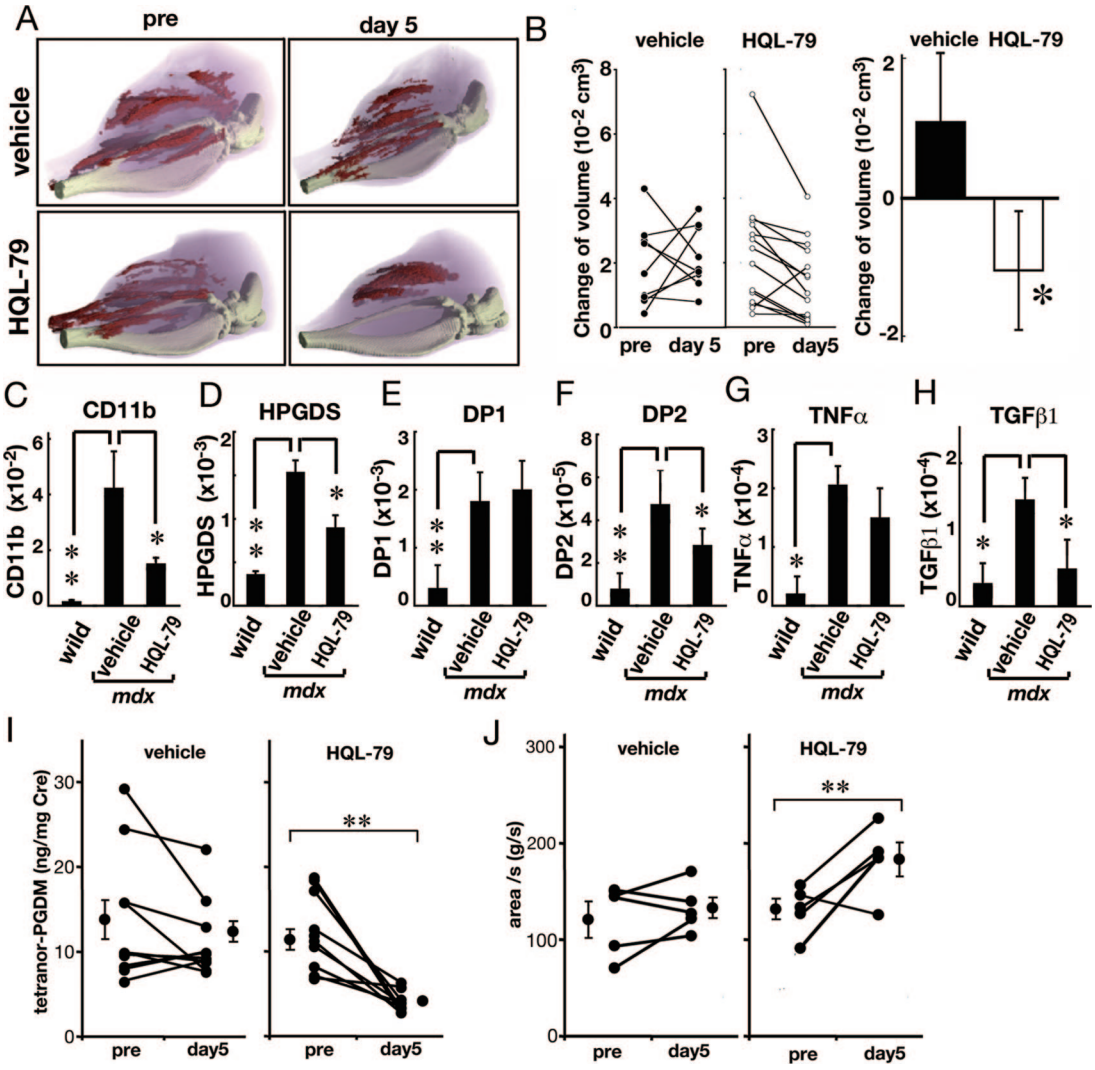

Figure 5. Reduction in the necrotic muscle volume and inflammation in the muscle from *mdx* mice by treatment with the HPGDS inhibitor HQL-79. **A:** Representative three-dimensional imaging of muscle necrosis in *mdx* mouse before and after treatment with vehicle or HQL-79 for 5 days. light pink: total muscle, red: enhanced muscle. **B: Left** panel shows changes in the volume of necrosis in individual *mdx* mice. **Right** panel summarizes changes in volume of necrosis. Necrotic Vehicle; $n = 9$, HQL-79; $n = 14$. **C–H:** Quantitative RT–PCR for mRNAs of CD11b, HPGDS, DP1, DP2, TNFα, and TGFβ1 in the muscle from wild-type and *mdx* mice after treatment with vehicle or HQL-79. Data are the mean ± SE. $n = 6$ in each group. $^{*}P < 0.05$. $^{**}P < 0.01$. **I:** Amount of tetranor-PGDM in the urine of *mdx* mice before and after HQL-79 administration. $n = 12$ and $n = 11$ in vehicle-treated and HQL-79 treated *mdx* mice, respectively. $^{**}P < 0.0003$. **J:** Grip strength test for *mdx* mice before and after HQL-79 administration. $n = 5$ in each group. $^{**}P < 0.0003$.

induced muscle injury and *mdx* mice, we hardly found any of the HPGDS-positive opaque fibers that had been previously observed in patient with DMD and polymyositis.[11] Furthermore, in mouse muscle, regenerated muscle fibers contained strong HPGDS immunoreactivity in their nuclei and weak immunoreactivity in their cytoplasm; whereas we did not observe HPGDS-positive regenerating muscle fibers in patient with DMD and polymyositis.[11] The HPGDS-immunoreactivity in the regenerating mouse muscle fibers diminished along with maturation and/or diameter enlargement.

It is unclear how necrotic muscle fibers express HPGDS immunoreactivity. However, an apoptosis-like phenomenon has recently been reported to occur during muscle necrosis.[31,32] Mizutani and Ohno[33] also reported that caspase-3, which is related to mitochondrial-mediated apoptosis, was expressed in necrotic muscle fiber. Furthermore, Honda et al[34] reported that the expression of the caspase-12 gene is involved in the endoplasmic reticulum stress pathway and that the Bax, caspase-9, and caspase-3 genes are involved in the mitochondrial stress pathway in the *mdx* masseter muscle. These data suggest that apoptosis occur during degeneration of *mdx* muscle. From these lines of evidence, it is possible that HPGDS expression is induced in muscle fibers during apoptosis.

We reported earlier that HPGDS expression was observed in "grouped necrosis" in patients with DMD.[11] The grouping of necrotic fibers is characteristic of DMD, and the underlying mechanism for this grouped necrosis has been proposed to be mast cell-mediated myocytotoxicity[35] or vascular ischemia.[36,37] Since PGD_2 is actively produced and released by mast cells,[10] and also functions as a vasodilator, it may be involved in progression of

grouped necrosis via both of the causative mechanisms mentioned above. We demonstrated that overproduction of PGD_2 caused massive muscular necrosis after BPVC injection into hHPGDS-TG mice (Figure 2A). In these mice, the histology showed remarkable interstitial edema and increased cell infiltration. PGD_2 elicits its biological actions, such as augmentation of vascular permeability and inhibition of platelet aggregation, through binding to the Gs-coupled DP1 receptor.[23,38] Thus PGD_2/DP1 signaling may enhance the pathological process of muscular necrosis by increasing vascular permeability. In addition, PGD_2 also acts on a Gαi-coupled DP2 receptor and may thereby induce the chemotactic migration of of Th2 cells, eosinophils, basophils, and monocytes to the necrotic fibers.[14] The increase in inflammatory cell infiltration into the necrotic area may contribute to augmentation of the inflammatory process. We demonstrated that the muscle necrosis tended to be affected by the antagonists for DP1 and DP2 but was efficiently suppressed by the HPGDS inhibitor, suggesting that both of these receptors are involved in augmented inflammatory responses in the muscular necrosis. Furthermore, as shown Figure 1, DP1 and DP2 receptors were up-regulated biphasically in BPVC-induced muscle necrosis. It is, therefore, possible that DP1 and DP2 receptors are involved in the regeneration of muscle fibers.

Therapeutic Implications of HPGDS Inhibitors in Muscle Necrosis

In this study, we demonstrated that HQL-79, an HPGDS inhibitor, suppressed PGD_2 production and improved muscle strength in the *mdx* mouse. The administration of corticosteroid to DMD patients was reported to produce clinical improvement.[5] Corticosteroid may cause the down-regulation of proteases and/or net increase in protein content.[39] Furthermore, the beneficial effects of corticosteroid may be due to suppression of cytosolic phospholipase A_2 and cyclooxygenase, which lead to the overall inhibition of PG synthesis.[40] However, the long-term administration of corticosteroids leads to serious side effects. Additionally, corticosteroids inhibit the production of cytoprotective prostanoids including prostaglandin E_2,[41] which is important in healing and muscle regeneration after injury. From these lines of evidence, it is theoretically advantageous to treat muscle necrosis focusing specifically on PGD_2 production and signaling.

Shen et al[42] mentioned that the decision to use nonsteroidal anti-inflammatory drugs, which are inhibitors of cyclooxygenase, to treat the muscle injuries warrants critical evaluation, because nonsteroidal anti-inflammatory drugs might impair muscle healing by inhibiting the fusion of myogenic precursor cells. In this study, we found that HPGDS was also expressed in the regenerating muscle in the early phase of regeneration, although the role of HPGDS in muscular regeneration remains to be clarified.

The molecular and enzymatic properties of HPGDS have been well characterized by us and other groups.[43] The crystal structure of HPGDS has already been determined.[43] The crystal structures of rat HPGDS,[43] human HPGDS,[44] and the complex of human HPGDS and HQL-79[19] have already been determined. Based on the crystallographic structure of the human HPGDS-HQL-79 complex, new HPGDS inhibitors are being designed by several pharmaceutical companies to be more potent and selective toward HPGDS. As we demonstrated here, since PGD_2 augmented the muscle necrosis in BPVC-induced necrosis and *mdx* mice, the suppression of PGD_2 production by HPGDS inhibitors may be beneficial for the treatment of DMD. Furthermore, because we reported previously that HPGDS expression is detectable in the muscle of polymyositis patients,[11] such HPGDS inhibitors may be predicted to be effective also for the treatment of polymyositis.

Acknowledgments

We thank Ms. Shigeko Matsumoto, Osaka Bioscience Institute, for conducting the immunocytochemistry; Ms. Yumiko Hoshikawa and Masumi Sakata, Osaka Bioscience Institute, for technical assistance; Dr. Hiroshi Yamamoto, Osaka University, for providing *mdx* mice; Dr. Tenjo Konishi and Dr. Norio Nakamura, Doshisha Women's College of Liberal Arts, for supporting the measurement of tetranor–PGDM by LC-MS/MS; and Mr. Masaki Kobayashi and Mr. Hiroshi Shigeta, ALOKA Co. Ltd., for CT analyses.

References

1. Emery AE: Muscular dystrophy into the new millennium. Neuromuscul Disord 2002, 12:343–349
2. Petrof BJ: The molecular basis of activity-induced muscle injury in Duchenne muscular dystrophy. Mol Cell Biochem 1998, 179:111–123
3. Kunkel LM, Monaco AP, Hoffman E, Koenig M, Feener C, Bertelson C: Molecular studies of progressive muscular dystrophy (Duchenne). Enzyme 1987, 38:72–75
4. Koenig M, Hoffman EP, Bertelson CJ, Monaco AP, Feener C, Kunkel LM: Complete cloning of the Duchenne muscular dystrophy (DMD) cDNA and preliminary genomic organization of the DMD gene in normal and affected individuals. Cell 1987, 50:509–517
5. Manzur AY, Kuntzer T, Pike M, Swan A: Glucocorticoid corticosteroids for Duchenne muscular dystrophy. Cochrane Database Syst Rev 2004, CD003725
6. Yilmaz O, Karaduman A, Topaloglu H: Prednisolone therapy in Duchenne muscular dystrophy prolongs ambulation and prevents scoliosis. Eur J Neurol 2004, 11:541–544
7. Biggar WD, Gingras M, Fehlings DL, Harris VA, Steele CA: Deflazacort treatment of Duchenne muscular dystrophy. J Pediatr 2001, 138:45–50
8. Tidball JG, Wehling-Henricks M: Evolving therapeutic strategies for Duchenne muscular dystrophy: targeting downstream events. Pediatr Res 2004, 56:831–841
9. Muntoni F, Fisher I, Morgan JE, Abraham D: Steroids in Duchenne muscular dystrophy: from clinical trials to genomic research. Neuromuscul Disord 2002, 12 Suppl 1:S162–S165
10. Urade Y, Ujihara M, Horiguchi Y, Igarashi M, Nagata A, Ikai K, Hayaishi O: Mast cells contain spleen-type prostaglandin D synthetase. J Biol Chem 1990, 265:371–375
11. Okinaga T, Mohri I, Fujimura H, Imai K, Ono J, Urade Y, Taniike M: Induction of hematopoietic prostaglandin D synthase in hyalinated necrotic muscle fibers: its implication in grouped necrosis. Acta Neuropathol 2002, 104:377–384
12. Mohri I, Taniike M, Taniguchi H, Kanekiyo T, Aritake K, Inui T, Fuku-

moto N, Eguchi N, Kushi A, Sasai H, Kanaoka Y, Ozono K, Narumiya S, Suzuki K, Urade Y: Prostaglandin D2-mediated microglia/astrocyte interaction enhances astrogliosis and demyelination in twitcher. J Neurosci 2006, 26:4383–4393
13. Hirata M, Kakizuka A, Aizawa M, Ushikubi F, Narumiya S: Molecular characterization of a mouse prostaglandin D receptor and functional expression of the cloned gene. Proc Natl Acad Sci USA: 1994, 91:11192–11196
14. Hirai H, Tanaka K, Yoshie O, Ogawa K, Kenmotsu K, Takamori Y, Ichimasa M, Sugamura K, Nakamura M, Takano S, Nagata K: Prostaglandin D2 selectively induces chemotaxis in T helper type 2 cells, eosinophils, and basophils via seven-transmembrane receptor CRTH2. J Exp Med 2001, 193:255–261
15. Urade Y, Hayaishi O: Prostaglandin D synthase: structure and function. Vitam Horm 2000, 58:89–120
16. Nonaka I, Takagi A, Ishiura S, Nakase H, Sugita H: Pathophysiology of muscle fiber necrosis induced by bupivacaine hydrochloride (Marcaine). Acta Neuropathol 1983, 60:167–174
17. Pinzar E, Miyano M, Kanaoka Y, Urade Y, Hayaishi O: Structural basis of hematopoietic prostaglandin D synthase activity elucidated by site-directed mutagenesis. J Biol Chem 2000, 275:31239–31244
18. Takemitsu M, Arahata K, Nonaka I: [Muscle regeneration in mdx mouse, and a trial of normal myoblast transfer into regenerating dystrophic muscle]. Rinsho Shinkeigaku 1990, 30:1066–1072
19. Aritake K, Kado Y, Inoue T, Miyano M, Urade Y: Structural and functional characterization of HQL-79, an orally selective inhibitor of human hematopoietic prostaglandin D synthase. J Biol Chem 2006, 281:15277–15286
20. Giles H, Leff P, Bolofo ML, Kelly MG, Robertson AD: The classification of prostaglandin DP-receptors in platelets and vasculature using BW A868C, a novel, selective and potent competitive antagonist. Br J Pharmacol 1989, 96:291–300
21. Sugimoto H, Shichijo M, Iino T, Manabe Y, Watanabe A, Shimazaki M, Gantner F, Bacon KB: An orally bioavailable small molecule antagonist of CRTH2, ramatroban (BAY u3405), inhibits prostaglandin D2-induced eosinophil migration in vitro. J Pharmacol Exp Ther 2003, 305:347–352
22. Mohri I, Eguchi N, Suzuki K, Urade Y, Taniike M: Hematopoietic prostaglandin D synthase is expressed in microglia in the developing postnatal mouse brain. Glia 2003, 42:263–274
23. Mizoguchi A, Eguchi N, Kimura K, Kiyohara Y, Qu WM, Huang ZL, Mochizuki T, Lazarus M, Kobayashi T, Kaneko T, Narumiya S, Urade Y, Hayaishi O: Dominant localization of prostaglandin D receptors on arachnoid trabecular cells in mouse basal forebrain and their involvement in the regulation of non-rapid eye movement sleep. Proc Natl Acad Sci USA: 2001, 98:11674–11679
24. Springer TA: Adhesion receptors of the immune system. Nature 1990, 346:425–434
25. Butcher EC: Warner-Lambert/Parke-Davis Award Lecture. Cellular and molecular mechanisms that direct leukocyte traffic. Am J Pathol 1990, 136:3–11
26. Hamer PW, McGeachie JM, Davies MJ, Grounds MD: Evans Blue Dye as an in vivo marker of myofibre damage: optimising parameters for detecting initial myofibre membrane permeability. J Anat 2002, 200:69–79
27. Matsuda R, Nishikawa A, Tanaka H: Visualization of dystrophic muscle fibers in mdx mouse by vital staining with Evans blue: evidence of apoptosis in dystrophin-deficient muscle. J Biochem 1995, 118:959–964
28. Song WL, Wang M, Ricciotti E, Fries S, Yu Y, Grosser T, Reilly M, Lawson JA, FitzGerald GA: Tetranor PGDM, an abundant urinary metabolite reflects biosynthesis of prostaglandin D2 in mice and humans. J Biol Chem 2008, 283:1179–1188
29. Matsushita N, Hizue M, Aritake K, Hayashi K, Takada A, Mitsui K, Hayashi M, Hirotsu I, Kimura Y, Tani T, Nakajima H: Pharmacological studies on the novel antiallergic drug HQL-79: i. Antiallergic and antiasthmatic effects in various experimental models. Jpn J Pharmacol 1998, 78:1–10
30. Matsushita N, Aritake K, Takada A, Hizue M, Hayashi K, Mitsui K, Hayashi M, Hirotsu I, Kimura Y, Tani T, Nakajima H: Pharmacological studies on the novel antiallergic drug HQL-79: iI. Elucidation of mechanisms for antiallergic and antiasthmatic effects. Jpn J Pharmacol 1998, 78:11–22
31. Graeber MB, Moran LB: Mechanisms of cell death in neurodegenerative diseases: fashion, fiction, and facts. Brain Pathol 2002, 12:385–390
32. Mattson MP: Apoptosis in neurodegenerative disorders. Nat Rev Mol Cell Biol 2000, 1:120–129
33. Mizutani M, Ohno N: Existence of apoptosis related proteins in the mdx mouse masseter muscle. Oral Med Pathol 2005, 10:1–7
34. Honda A, Abe S, Hiroki E, Honda H, Iwanuma O, Yanagisawa N, Ide Y: Activation of caspase 3, 9, 12, and Bax in masseter muscle of mdx mice during necrosis. J Muscle Res Cell Motil 2007, 28:243–247
35. Gorospe JR, Tharp M, Demitsu T, Hoffman EP: Dystrophin-deficient myofibers are vulnerable to mast cell granule-induced necrosis. Neuromuscul Disord 1994, 4:325–333
36. Mendell JR, Engel WK, Derrer EC: Duchenne muscular dystrophy: functional ischemia reproduces its characteristic lesions. Science 1971, 172:1143–1145
37. Asai A, Sahani N, Kaneki M, Ouchi Y, Martyn JA, Yasuhara SE: Primary role of functional ischemia, quantitative evidence for the two-hit mechanism, and phosphodiesterase-5 inhibitor therapy in mouse muscular dystrophy. PLoS ONE 2007, 2:e806
38. Narumiya S, Sugimoto Y, Ushikubi F: Prostanoid receptors: structures, properties, and functions. Physiol Rev 1999, 79:1193–1226
39. Haycock JW, Falkous G, Maltin CA, Delday MI, Mantle D: Effect of prednisone on protease activities and structural protein levels in rat muscles in vivo. Clin Chim Acta 1996, 249:47–58
40. Masferrer JL, Seibert K, Zweifel B, Needleman P: Endogenous glucocorticoids regulate an inducible cyclooxygenase enzyme. Proc Natl Acad Sci USA: 1992, 89:3917–3921
41. Tanaka H, Watanabe K, Tamaru N, Yoshida M: Arachidonic acid metabolites and glucocorticoid regulatory mechanism in cultured porcine tracheal smooth muscle cells. Lung 1995, 173:347–361
42. Shen W, Li Y, Tang Y, Cummins J, Huard J: NS-398, a cyclooxygenase-2-specific inhibitor, delays skeletal muscle healing by decreasing regeneration and promoting fibrosis. Am J Pathol 2005, 167:1105–1117
43. Kanaoka Y, Ago H, Inagaki E, Nanayama T, Miyano M, Kikuno R, Fujii Y, Eguchi N, Toh H, Urade Y, Hayaishi O: Cloning and crystal structure of hematopoietic prostaglandin D synthase. Cell 1997, 90:1085–1095
44. Inoue T, Irikura D, Okazaki N, Kinugasa S, Matsumura H, Uodome N, Yamamoto M, Kumasaka T, Miyano M, Kai Y, Urade Y: Mechanism of metal activation of human hematopoietic prostaglandin D synthase. Nat Struct Biol 2003, 10:291–296